A space elevator deployed at the L1 Mars-Phobos libration point

Vladimir S. Aslanov

Moscow Aviation Institute (National Research University), 4, Volokolamskoe Shosse, A-80, GSP-3, Moscow, Russia

+7-9276889791

aslanov_vs@mail.ru

http://aslanov.ssau.ru/

Abstract The paper investigates the feasibility of designing and deploying a space elevator fixed at the L1 libration point in the Mars-Phobos system in the framework of the planar circular restricted three-body problem. Two configurations of the space elevator are discussed. One is directed towards Phobos and the other towards Mars. In the first case, the length of the elevator is limited by the distance to the surface of Phobos (about 3.4 km), and in the second by the distance to the surface of Mars (about 7800 km). The law of motion of the climber is proposed, including the acceleration part, the braking part and the main part of the climbing (or descending) of the climber at constant velocity. The influence of the mass ratio of the climber and the end body is analyzed. It is also shown that it is possible to turn the elevator 180 degrees from the direction of Phobos to the direction of Mars and back when the climber is at the end point of the elevator. This is achieved using the well-known control law of the elevator length. This is the first preliminary study on the design of the Mars-Phobos space elevator using the L1 libration point, based on theoretical statements and numerical simulation results.

Keywords *L1 libration point · Mars-Phobos system · Space elevator · Control law · Equations of motion.*

1 Introduction

Space tethers and their variety of space elevators can be used in many future space missions as an economical and simple alternative to propulsion systems. An invaluable contribution to developing and popularising space tether systems was made by Beletsky and Levin [1]. The space elevator concept was proposed by Tsiolkovsky [2] in the 19th century. The modern design of a space elevator was presented by Artsutanov [3] and the theoretical possibility of building an orbital tower for a geostationary Earth satellite was proposed by Pearson [4]. The basis of a classic space elevator is a tether about 100,000 km long attached to the Earth's surface. At the moment, at least, it's science fiction. Cohen and Misra [5] proposed to consider the use of a partial elevator - shorter in length and floating in space. The idea of a partial space lift was subsequently developed in later works by Misra et al [6-8] and works by Zhu et al [9-12]. So far, hundreds of scientific works (for example [13-18]) have been published on the possibility of using space tethers. One of the promising areas for the practical application of space tethers and elevators is the study of the far Solar System planets and their moons.

Among the projects related to the use of tether systems for the study of planets and moons, NASA's the Phobos L1 Operational Tether Experiment (PHLOTE) deserves a special mention [19]. The PHLOTE mission focuses on studying the surface of Phobos using a tether deployed from an orbiting spacecraft located at the L1 libration point of the Mars-Phobos system. The L1 libration point is about 3.4 km from the surface of Phobos. Scientific instruments are placed at the end of the tether and are used to study the surface of Phobos from a low altitude. Some of the ideas of the PHLOTE mission are developed in the paper [20].The PHLOTE mission set the stage for the design of a space elevator to be attached to the L1 libration point of the Mars-Phobos system. In the proposed space elevator, the tether is attached at the L1 libration point, the end mass is placed at the free end, and the climber moves along the tether as on a cableway. In static position, this space elevator is a double pendulum, which is studied in the paper [21]. The goal of this paper is to study the feasibility of designing and deploying a space elevator attached at the L1 libration point of the Mars-Phobos system in the framework of the planar circular restricted three-body problem.

Two configurations of the space elevator are discussed. One is directed towards Phobos and the other towards Mars. In the first case, the length of the elevator is limited by the distance to the surface of Phobos (about 3.4 km), and in the second case it is restricted by the distance to the surface of Mars (about 7800 km). The control law of the climber motion is proposed, including the acceleration part, the braking part and the main part of the climbing (or descending) at constant velocity. The influence of the mass ratio of the climber and the end body is analyzed. It is also shown that it is possible to turn the elevator 180 degrees from the direction of Phobos to the direction of Mars and back when the climber is at the end point of the elevator. This is achieved by using the well-known control law of the elevator length. This is the first preliminary study on the design of the Mars-Phobos space elevator using the L1 libration point, based on theoretical statements and numerical simulation results.

The objective of the paper is achieved in four phases:

1. The basic assumptions are formulated in the framework of the circular plane restricted three-body problem, and the equations of motion of the space elevator attached to the L1 libration point are derived in polar coordinates.
2. The control law of the climber motion including accelerating, main and braking phases is proposed.

3. For two cases, where the space elevator is deployed towards Phobos and towards Mars, the motion of the climber in two opposite directions is analyzed.
4. The possibility of turning the space elevator from Phobos to Mars direction and back has been studied.

2 Motion equations of the space elevator

In this section the equations of plane motion of a space elevator in gravitational fields of two primaries (Mars-Phobos) in rotating polar coordinates with respect to the L1 libration point are derived in the framework of the circular restricted three-body problem [22].

2.1 Key assumptions

The following acceptable assumptions are introduced:

1. It is supposed that the primaries move in circular orbits around their mutual mass center (point O in Fig. 1).

2. The space elevator is considered as a double pendulum. The end masses of the pendulums m_1 (the climber) and m_2 (the end mass) are significantly smaller than the primary masses M_1 and M_2

$$m_1,\, m_2 \ll M_2 < M_1 \tag{1}$$

3. The pendulums consist of weightless rigid rods of variable length l_1, l_2.

4. In the circular restricted three-body problem, the mean rotation is

$$\omega = \frac{df}{dt} = const \tag{2}$$

where f is the true anomaly.

5. In all considered cases, only in-plane motion is studied.

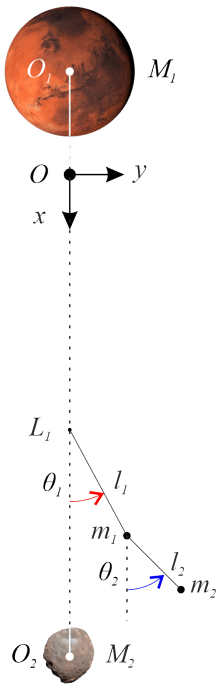

Fig. 1 The frame Oxy

2.2 Motion equations of a space elevator attached at the L1 libration point

Consider the equations of the end mass planar motion in the Local-Vertical-Local-Horizontal frame Oxy within the scope of the classical restricted three-body problem [22]

$$m_1\left(\ddot{x}_1-\omega^2 x_1-2\omega\dot{y}_1\right)=\frac{\partial U}{\partial x_1}-T_1\cos\theta_1+T_2\cos\theta_2 \tag{3}$$

$$m_1\left(\ddot{y}_1-\omega^2 y_1+2\omega\dot{x}_1\right)=\frac{\partial U}{\partial y_1}-T_1\sin\theta_1+T_2\sin\theta_2 \tag{4}$$

$$m_2\left(\ddot{x}_2-\omega^2 x_2-2\omega\dot{y}_2\right)=\frac{\partial U}{\partial x_2}-T_2\cos\theta_2 \tag{5}$$

$$m_2\left(\ddot{y}_2-\omega^2 y_2+2\omega\dot{x}_2\right)=\frac{\partial U}{\partial y_2}-T_2\sin\theta_2 \tag{6}$$

where ω is mean orbital rate, T_1 and T_2 are the tensions in tether l_1 and l_2, respectively. The potential of Eqs. (3) and (4) is written as

$$U(x_1,y_1,x_2,y_2)=G\left(\frac{m_1M_1}{r_{11}}+\frac{m_1M_2}{r_{12}}+\frac{m_2M_1}{r_{21}}+\frac{m_2M_2}{r_{22}}\right) \tag{7}$$

where G is Newtonian gravitational constant, the distances between the primaries (1 and 2) and the climber and the end mass (Fig. 1)

$$r_{11}=\sqrt{(x_1+d\mu)^2+y_1^{\,2}} \tag{8}$$

$$r_{12}=\sqrt{(x_1-d(1-\mu))^2+y_1^{\,2}} \tag{9}$$

$$r_{21} = \sqrt{(x_2 + d\mu)^2 + y_2^{\;2}} \tag{10}$$

$$r_{22} = \sqrt{(x_2 - d(1-\mu))^2 + y_2^{\;2}} \tag{11}$$

where d is the distance between the primaries 1 and 2, $\mu = \dfrac{m_2}{m_1 + m_2}$ is the mass ratio.

The change to the polar coordinates by means of substitution of the variables

$$x_1 = a + l_1 = \cos\theta_1,\; y_1 = l_1 \sin\theta_1\,, \tag{12}$$

$$x_2 = a + l_1\cos\theta_1 + l_2\cos\theta_2,\; y_2 = l_1\sin\theta_1 + l_2\sin\theta_2 \tag{13}$$

leads to Eqs. (3)-(6) in the following form

$$l_1\ddot{\theta}_1 = G\left[\frac{M_1\rho_1\sin\theta_1}{r_{11}^{\;3}} + \frac{M_2\rho_2\sin\theta_1}{r_{12}^{\;3}}\right] - a\omega^2\sin\theta_1 - 2\dot{l}_1\left(\omega + \dot{\theta}_1\right) - \frac{T_2}{m_1}\sin\theta_{12} \tag{14}$$

$$l_2\ddot{\theta}_2 = G\left[\frac{\left(r_{12}^{\;3} - r_{22}^{\;3}\right)M_2\left(\rho_2\sin\theta_2 - \sin\theta_{12}l_1\right)}{r_{12}^{\;3}r_{22}^{\;3}} + \frac{\left(r_{11}^{\;3} - r_{21}^{\;3}\right)M_1\left(\rho_1\sin\theta_2 - \sin\theta_{12}l_1\right)}{r_{11}^{\;3}r_{21}^{\;3}}\right] -$$

$$2\dot{l}_2\left(\omega + \dot{\theta}_2\right) + \frac{T_1}{m_1}\sin\theta_{12}\,, \tag{15}$$

$$\ddot{l}_1 = -G\left[\frac{M_1\left(\rho_1\cos\theta_1 + l_1\right)}{r_{11}^{\;3}} + \frac{M_2\left(\rho_2\cos\theta_1 + l_1\right)}{r_{12}^{\;3}}\right] + a\omega^2\cos\theta_1 + l_1\left(\omega + \dot{\theta}_1\right)^2 + \frac{1}{m_1}\left(T_2\cos\theta_{12} - T_1\right) \tag{16}$$

$$\ddot{l}_2 = -G\left[\frac{M_1\left(\left(r_{11}^{\;3} - r_{21}^{\;3}\right)\left(\rho_1\cos\theta_2 + l_1\cos\theta_{12}\right) + r_{11}^{\;3}l_2\right)}{r_{11}^{\;3}r_{21}^{\;3}} +\right.$$

$$\left.\frac{M_2\left(\left(r_{12}^{\;3} - r_{22}^{\;3}\right)\left(\rho_2\cos\theta_2 + \cos\theta_{12}l_1\right) + r_{12}^{\;3}l_2\right)}{r_{12}^{\;3}r_{22}^{\;3}}\right] + l_2\left(\omega + \dot{\theta}_2\right)^2 - \left(\frac{1}{m_1} + \frac{1}{m_2}\right)T_2 + \frac{T_1}{m_1}\cos\theta_{12} \tag{17}$$

where

$$r_{11} = \sqrt{\rho_1^{\;2} + 2\rho_1 l_1\cos\theta_1 + l_1^2}\quad, \tag{18}$$

$$r_{12} = \sqrt{\rho_2^{\;2} + 2\rho_2 l_1\cos\theta_1 + l_1^{\;2}}\,, \tag{19}$$

$$r_{21} = \sqrt{(\rho_1 + l_1\cos\theta_1 + l_2\cos\theta_2)^2 + (l_1\sin\theta_1 + l_2\sin\theta_2)^2}\;, \tag{20}$$

$$r_{22} = \sqrt{(\rho_2 + l_1\cos\theta_1 + l_2\cos\theta_2)^2 + (l_1\sin\theta_1 + l_2\sin\theta_2)^2}\;, \tag{21}$$

$$\rho_1 = a + d\mu\,,\; \rho_2 = a - d(1-\mu) \tag{22}$$

Here a is the coordinate of the L1 libration point in the frame Oxy, θ_1 and θ_2 are deflection angles of the space elevator (Fig.1), $\theta_{12} = \theta_1 - \theta_2$.

The behaviour of the space elevator depends on the tether tension T_1 and T_2 , which are included in the right-hand sides of Eqs. (14)-(17). In the case when the tether lengths are given as functions of time $l_1(t)$ and $l_2(t)$, then the tether tension can be found by solving Eqs. (16) and (17) with respect to T_1 and T_2, as follows

$$T_1 = \frac{m_1 m_2}{m_1 + m_2 \sin\theta_{12}^2}\Bigg[GM_1\left(-\frac{(l_1+\rho_1\cos\theta_1)}{\mu r_{11}^3} - \cos\theta_{12}\left(-\frac{\rho_1\cos\theta_2 + l_1\cos\theta_{12}}{r_{11}^3} + \frac{\rho_1\cos\theta_2 + l_1\cos\theta_{12} + l_2}{r_{21}^3}\right)\right)+$$

$$GM_2\left(-\frac{(l_1+\rho_2\cos\theta_1)}{\mu r_{12}^3} - \cos\theta_{12}\left(-\frac{\rho_2\cos\theta_2 + l_1\cos\theta_{12}}{r_{12}^3} + \frac{\rho_2\cos\theta_2 + l_1\cos\theta_{12} + l_2}{r_{22}^3}\right)\right)+$$

$$\frac{1}{\mu}\left(a\omega^2\cos\theta_1 + l_1\left(\omega+\dot{\theta}_1\right)^2 - \ddot{l}_1\right) + l_2\cos\theta_{12}\left(\omega+\dot{\theta}_2\right)^2 - \cos\theta_{12}\ddot{l}_2\Bigg], \tag{23}$$

$$T_2 = \frac{m_1 m_2}{m_1 + m_2 \sin\theta_{12}^2}\Bigg[GM_1\left(\frac{\rho_1\sin\theta_1\sin\theta_{12}}{r_{11}^3} - \frac{\rho_1\cos\theta_2 + l_1\cos\theta_{12} + l_2}{r_{21}^3}\right)+$$

$$GM_2\left(\frac{\rho_2\sin\theta_1\sin\theta_{12}}{r_{12}^3} - \frac{\rho_2\cos\theta_2 + l_1\cos\theta_{12} + l_2}{r_{22}^3}\right)+$$

$$\frac{a\omega^2}{2}\left(\cos(2\theta_1-\theta_2) + \cos\theta_2\right) + l_1\left(\omega+\dot{\theta}_1\right)^2\cos\theta_{12} + l_2\left(\omega+\dot{\theta}_2\right)^2 - \ddot{l}_1\cos\theta_{12} - \ddot{l}_2\Bigg] \tag{24}$$

3 Accelerating, main and braking phases

3.1 Climbing at constant velocity

Assume the climber m_1 moves at a constant velocity

$$\dot{l}_1 = V = const \quad \dot{l}_2 = -V = const \quad \ddot{l}_1 = 0\,,\ \ddot{l}_2 = 0 \tag{25}$$

It is assumed that the total length of the tether is constant, and therefore

$$l_0 = l_1 + l_2 = const\,,\ l_1 = l_0 + Vt\,, l_2 = -Vt \tag{26}$$

Substituting (25) into Eqs. (14), (15), (23) and (24), get

$$\ddot{\theta}_1 = \frac{1}{l_1}\left[G\left(\frac{M_1\rho_1\sin\theta_1}{r_{11}{}^3} + \frac{M_2\rho_2\sin\theta_1}{r_{12}{}^3}\right) - a\omega^2\sin\theta_1 - 2V\left(\omega+\dot{\theta}_1\right) - \frac{T_2}{m_1}\sin\theta_{12}\right], \tag{27}$$

$$\ddot{\theta}_2 = \frac{1}{l_2}\left[G\left(\frac{\left(r_{12}{}^3 - r_{22}{}^3\right)M_2\left(\rho_2\sin\theta_2 - \sin\theta_{12}l_1\right)}{r_{12}{}^3 r_{22}{}^3} + \frac{\left(r_{11}{}^3 - r_{21}{}^3\right)M_1\left(\rho_1\sin\theta_2 - \sin\theta_{12}l_1\right)}{r_{11}{}^3 r_{21}{}^3}\right)+\right.$$

$$2V\left(\omega+\dot{\theta}_2\right)+\frac{T_1}{m_1}\sin\theta_{12}\Bigg] \qquad (28)$$

where

$$T_1=\frac{m_1m_2}{m_1+m_2\sin\theta_{12}{}^2}\Bigg[GM_1\left(-\frac{(l_1+\rho_1\cos\theta_1)}{\mu r_{11}^3}-\cos\theta_{12}\left(-\frac{\rho_1\cos\theta_2+l_1\cos\theta_{12}}{r_{11}^3}+\frac{\rho_1\cos\theta_2+l_1\cos\theta_{12}+l_2}{r_{21}^3}\right)\right)+$$

$$GM_2\left(-\frac{(l_1+\rho_2\cos\theta_1)}{\mu r_{12}^3}-\cos\theta_{12}\left(-\frac{\rho_2\cos\theta_2+l_1\cos\theta_{12}}{r_{12}^3}+\frac{\rho_2\cos\theta_2+l_1\cos\theta_{12}+l_2}{r_{22}^3}\right)\right)+$$

$$\frac{1}{\mu}\left(a\omega^2\cos\theta_1+l_1\left(\omega+\dot{\theta}_1\right)^2\right)+l_2\cos\theta_{12}\left(\omega+\dot{\theta}_2\right)^2\Bigg], \qquad (29)$$

$$T_2=\frac{m_1m_2}{m_1+m_2\sin\theta_{12}{}^2}\Bigg[GM_1\left(\frac{\rho_1\sin\theta_1\sin\theta_{12}}{r_{11}^3}-\frac{\rho_1\cos\theta_2+l_1\cos\theta_{12}+l_2}{r_{21}^3}\right)+$$

$$GM_2\left(\frac{\rho_2\sin\theta_1\sin\theta_{12}}{r_{12}^3}-\frac{\rho_2\cos\theta_2+l_1\cos\theta_{12}+l_2}{r_{22}^3}\right)+$$

$$\frac{a\omega^2}{2}\left(\cos\left(2\theta_1-\theta_2\right)+\cos\theta_2\right)+l_1\left(\omega+\dot{\theta}_1\right)^2\cos\theta_{12}+l_2\left(\omega+\dot{\theta}_2\right)^2\Bigg] \qquad (30)$$

At the beginning or at the end of the climber's motion l_1 (or l_2) tends to zero, this leads to an increase in the amplitude of the tether oscillations, as follows from Eqs. (27) and (28). In practice, in this problem there are no material points for which these equations of motion are written, but rigid bodies with linear dimensions. This fact allows us to exclude singular points ($l_1=0$, $l_2=0$) from consideration. With the total length of the space elevator equal to $l_0=3400\,m$, the climber's motion starts from position

$l_1=l_0-\Delta_0=3399\,m$, $l_2=\Delta_0=1\,m$,

and ends at

$l_2=l_0-\Delta_f=3399.5\,m$, $l_1=\Delta_f=0.5\,m$

Fig. 2 plots the deflection angles of the tether θ_1 and θ_2 when the masses of the climber and the end body are equal $m_1=m_2=100\,kg$, the climber's velocity $V=-0.1\,m\,s^{-1}$, for the following initial conditions:

$$\theta_1=0.1\,rad\ ,\ \theta_2=-0.1\,rad\ ,\ \dot{\theta}_1=0\ ,\ \dot{\theta}_2=0 \qquad (31)$$

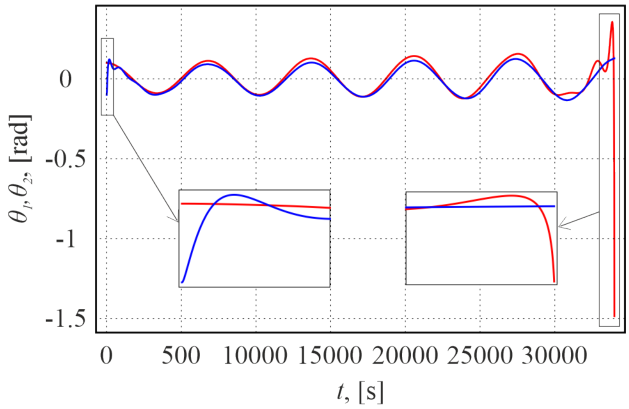

Fig. 2 The deflection angles of the space elevator θ_1 and θ_2

There is a sharp increase in the tether deflection angle θ_1 at the end of the ascent, as shown in Fig. 2.

3.2 Accelerating, main and braking phases

Obviously, the velocity of a climber cannot change instantaneously from zero to some finite value $V \neq 0$. Similarly, a climber cannot stop instantaneously. Therefore, the main phase of the climber's motion at constant velocity should be preceded by an acceleration phase and followed at the end by a deceleration phase. These three phases of motion look like this:

Accelerating phase $t \in (t_0, t_0 + t_V)$

$$l_1 = l_0 + \frac{4Vt_V}{\pi} \sin\left[\frac{\pi(t-t_0)}{4t_V}\right]^2, \qquad l_2 = l_0 - l_1, \tag{32}$$

$$V_1 = \frac{d}{dt} l_1 = V \sin\left[\frac{\pi(t-t_0)}{2t_V}\right], \qquad V_2 = -V_1,$$

$$W_1 = \frac{d}{dt} V_1 = \frac{\pi V}{2t_V} \cos\left[\frac{\pi(t-t_0)}{2t_V}\right], \qquad W_2 = -W_1$$

Main phase $t \in (t_0 + t_V, t_f - t_V)$

$$l_1 = l_0 + V\left[t - t_V\left(1 - \frac{2}{\pi}\right) - t_0\right], \qquad l_2 = l_0 - l_1, \tag{33}$$

$$V_1 = \frac{d}{dt} l_1 = V, \qquad V_2 = -V_1,$$

$$W_1 = \frac{d}{dt} V_1 = 0, \qquad W_2 = -W_1 = 0$$

Decelerating phase $t \in (t_f - t_V, t_f)$

$$l_1 = l_0 + \left(t_f - t_0 - 2t_V\right)V + \frac{4Vt_V}{\pi}\cos\left[\frac{\pi\left(t_f - t\right)}{4t_V}\right]^2, \qquad l_2 = l_0 - l_1, \tag{34}$$

$$V_1 = \frac{d}{dt}l_1 = V\sin\left[\frac{\pi\left(t_f - t\right)}{2t_V}\right], \qquad V_2 = -V_1,$$

$$W_1 = \frac{d}{dt}V_1 = -\frac{\pi V}{2t_V}\cos\left[\frac{\pi\left(t_f - t\right)}{2t_V}\right], \quad W_2 = -W_1 = 0$$

where t_0 and t_f are start and end times, t_V is the duration of the acceleration and deceleration phases, W_1 and W_2 are the accelerations. Fig. 3 shows the velocity profile of the climber $V_1 = \frac{d}{dt}l_1$.

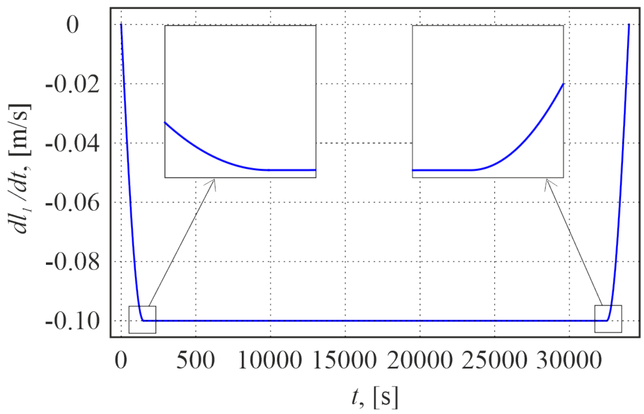

Fig. 3 The velocity profile of the climber $\frac{d}{dt}l_1(t) < 0$ for $m_1 = m_2 = 100kg$, $l = 3400m$ $t_V = 1500\,s$

4 Climbing from Phobos to the L1 libration point and reverse

4.1 Climbing from Phobos to the L1 libration point

Fig. 4 illustrates the behaviour of the space elevator when the climber moves according to the laws (32)-(34), the acceleration time and deceleration time are equal to $t_V = 1500\,s$. The space elevator parameters and initial motion conditions (31) are taken to be exactly the same as in the construction of Fig. 2.

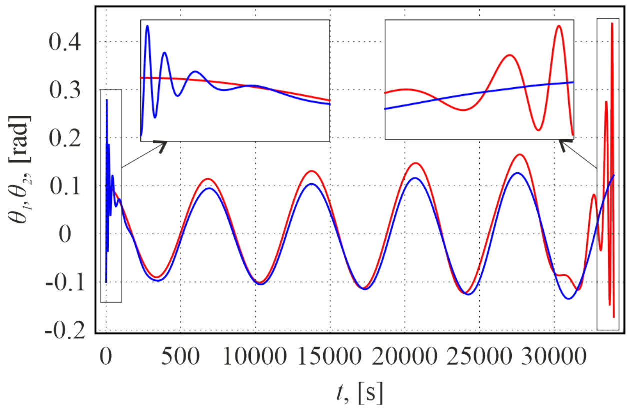

Fig. 4 The deflection angles of the space elevator θ_1 (red) and θ_2 (blue) for the laws (33)-(35) for $\sigma = \dfrac{m_2}{m_1} = 1$

Comparison of Fig. 2 and Fig. 4 shows that the application of the acceleration and deceleration phases of the climber (32) and (34), more than 3 times reduce the deflection angles of the space elevator at the beginning and end of the climber's motion. As Fig. 5 indicates, the forces in the tethers l_1 and l_2 do not exceed 0.4 N.

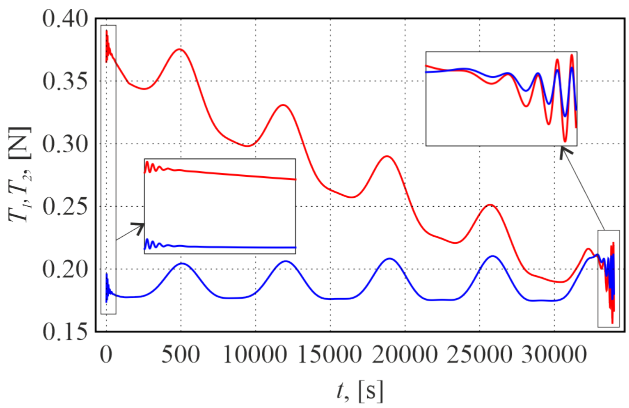

Fig. 5 The tether tension T_1 (red) and T_2 (blue) for $\sigma = \dfrac{m_2}{m_1} = 1$

4.2 Influence of the ratio of climber mass to end mass on the dynamics of the space elevator

The case when the mass ratio $\sigma = \frac{m_2}{m_1}$ equals 1 is illustrated in Figs. 4 and 5, where $m_1 = m_2 = 100\,kg$. Figs. 6 and 7 show the deflection angles θ_1 and θ_2, and the forces in the tethers l_1 and l_2, with the total mass of the space elevator unchanged

$$m_1 + m_2 = 200\,kg \tag{35}$$

a

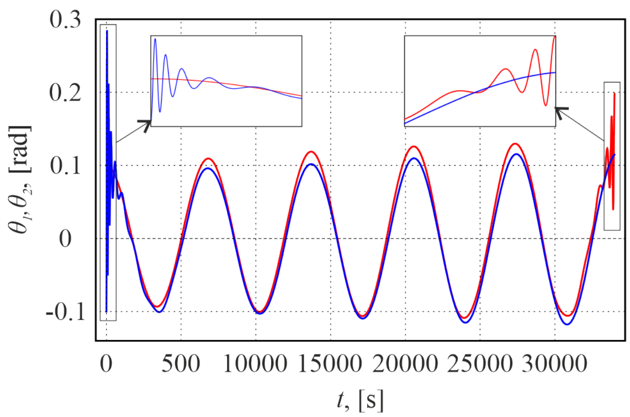

b

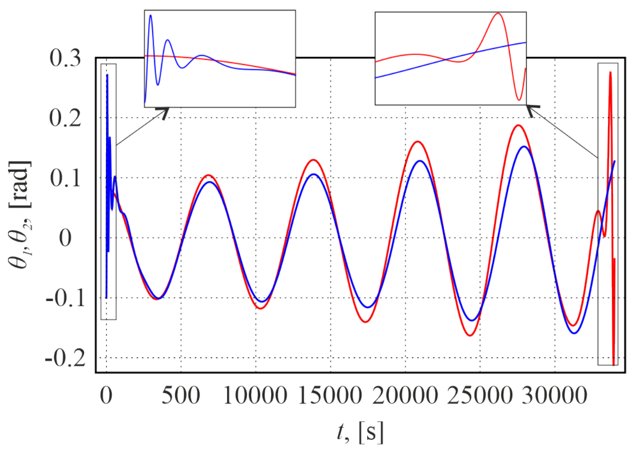

Fig. 6 The deflection angles of the space elevator θ_1 (red) and θ_2 (blue) for

(**a**) $\sigma = 2$ ($m_1 = 66.667kg$ $m_2 = 133.333kg$)

(**b**) $\sigma = 0.5$ ($m_1 = 133.333kg$ $m_2 = 66.667kg$)

a

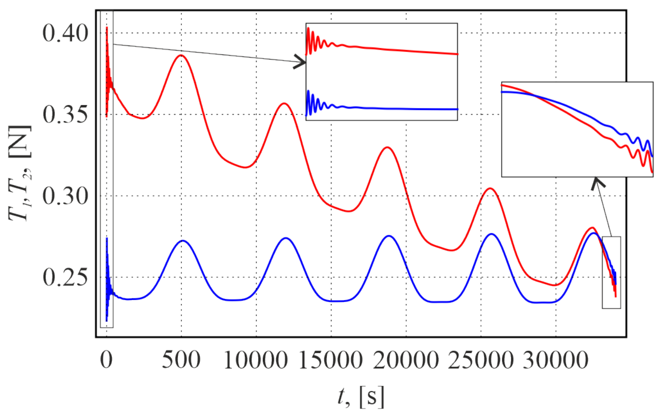

b

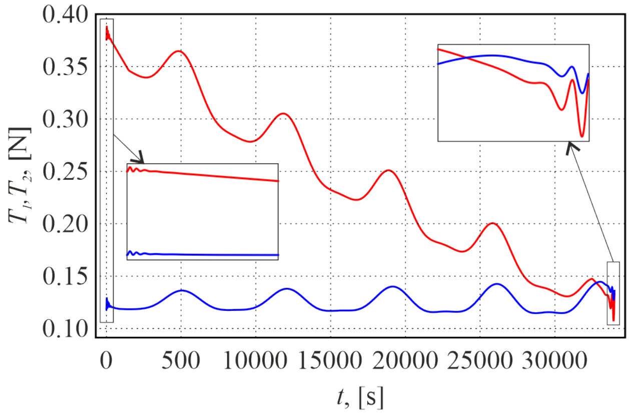

Fig. 7 The tether tension T_1 (red) and T_2 (blue) for $\sigma = 0.5$, $l = 3400m$

(**a**) $\sigma = 2$ ($m_1 = 66.667kg$ $m_2 = 133.333kg$)

(**b**) $\sigma = 0.5$ ($m_1 = 133.333kg$ $m_2 = 66.667kg$)

The simulation results presented in Figs .4 - 7 show that changing the mass ratio within the range $\sigma = \frac{m_2}{m_1} \notin [0.5, 2]$ does not essentially change the dynamics of the space elevator.

4.3 Descending from the L1 libration point to Phobos

Consider the dynamics of the equal-mass elevator ($\sigma = \frac{m_2}{m_1} = 1$) when descending from the L1 libration point to Phobos.

(**a**)

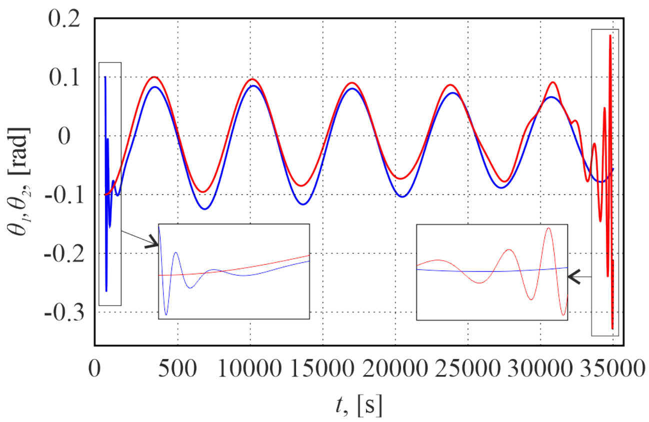

(**b**)

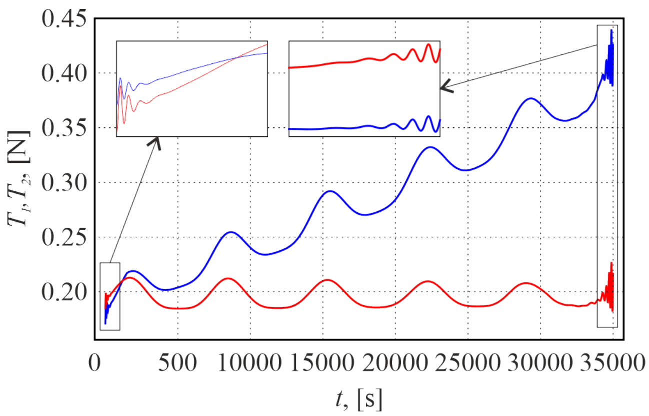

Fig. 8 (**a**) The deflection angles of the space elevator θ_1 (red) and θ_2 (blue), and

(**b**) the tether tension T_1 (red) and T_2 (blue) for $\sigma = \frac{m_2}{m_1} = 1$

Comparison of Figs .4 and 5 with Fig. 7 indicate the similarity of the simulation results presented for the climbing and descending of the climber.

5 Space elevator deployed towards Mars. Moving the climber to the L1 libration point and back

Consider the case where the space elevator is deployed from the L1 libration point towards Mars, as shown in Fig. 9. The same climber velocity control laws for the acceleration, main and braking phases (32)-(34) are used as before.

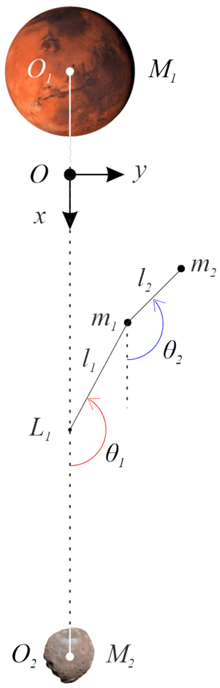

Fig. 9 The frame Oxy

As before, the velocity of the climber in the main phase is equal to $V = -0.1\, m\, s^{-1}$, the length of the elevator is equal to $l_0 = 3400\, m$, and the mass of the climber and the final mass are equal to $m_1 = m_2 = 100\, kg$. The initial conditions differ from the initial conditions (31) by the angle π:

$$\theta_1 = \pi + 0.1 rad \ , \ \theta_2 = \pi - 0.1 rad \ , \ \dot{\theta}_1 = 0 \ , \ \dot{\theta}_2 = 0 \qquad (36)$$

Figs. 10 and 11 show the angles of tether deflection θ_1 and θ_2 when the climber moves towards the L1 libration point and towards Mars, respectively.

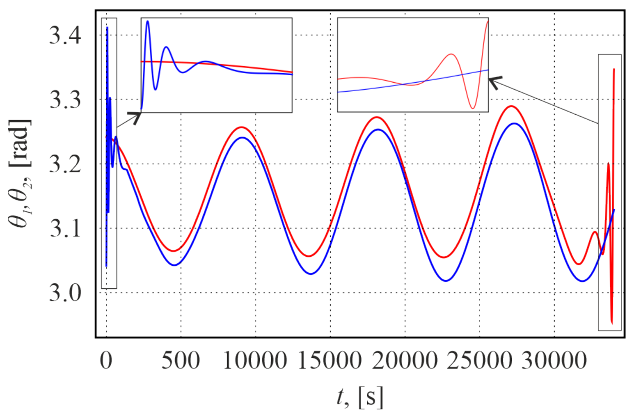

Fig. 10 The deflection angles of the space elevator θ_1 (red) and θ_2 (blue) for the climber

moving towards the L1 libration point

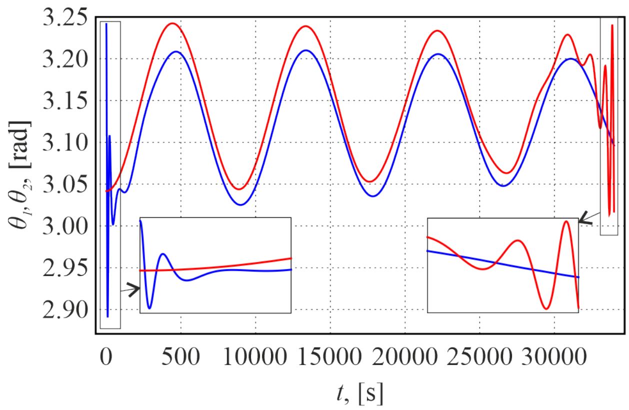

Fig. 11 The deflection angles of the space elevator θ_1 (red) and θ_2 (blue) for the climber moving towards Mars

As can be seen from Figs. 10 and 11, there is no essential difference in the direction in which the climber moves, the deflection angles only increase at the beginning or end of the motion.

6 Turning the elevator towards Mars and back

In the last section, we answer the question of whether it is possible to turn the space elevator attached to the L1 libration point from the direction of Phobos to the direction of Mars and vice versa. First, consider the case where the space elevator is turned towards Phobos and the climber is at the bottom point. The climber and end mass form a single body ($l_2 = 0$) with mass equal to $m = m_1 + m_2$. To turn the space elevator 180 degrees towards Mars, the tether length control law for $l = l_1$ from study [23] is used

$$l = l_0\left(1 + c\frac{d\theta}{dt}\sin\theta\right) \tag{37}$$

where l_0 is the initial tether length, c is the control dimensionless coefficient, $\theta = \theta_1$.

The equations of motion of the space elevator (14)-(17) are reduced to a single second order differential equation

$$l\ddot{\theta} = G\left[\frac{M_1\rho_1 \sin\theta}{r_{11}^{\ 3}} + \frac{M_2\rho_2 \sin\theta}{r_{12}^{\ 3}}\right] - a\omega^2 \sin\theta - 2\dot{l}\left(\omega + \dot{\theta}\right) \quad (38)$$

where

$$r_{11} = \sqrt{\rho_1^{\ 2} + 2\rho_1 l \cos\theta_1 + l^{\ 2}} \quad , \quad (39)$$

$$r_{12} = \sqrt{\rho_2^{\ 2} + 2\rho_2 l \cos\theta + l^{\ 2}} \ , \quad (40)$$

The time it takes for the space elevator to overturn depends on the dimensionless control coefficient and the initial conditions of the motion, which for the plot in Fig. 12 are taken as follows

$$c = -200 \ , \ \theta_0 = -0.2\, rad \ , \frac{d\theta_0}{dt} = 0 \quad (41)$$

(a)

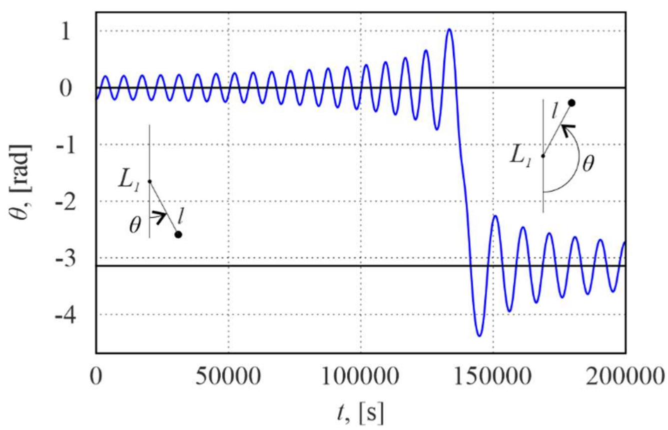

(b)

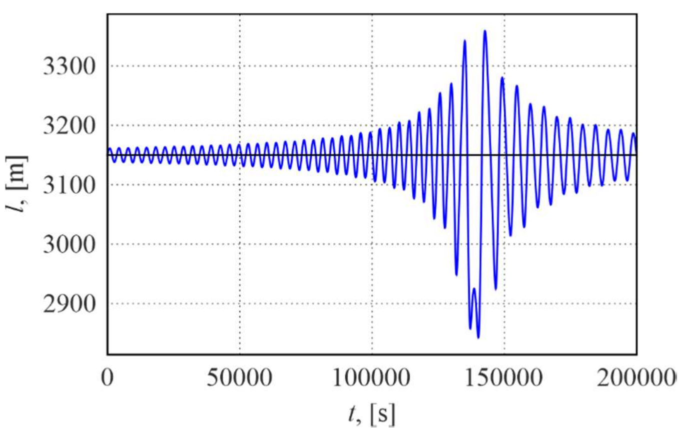

(c)

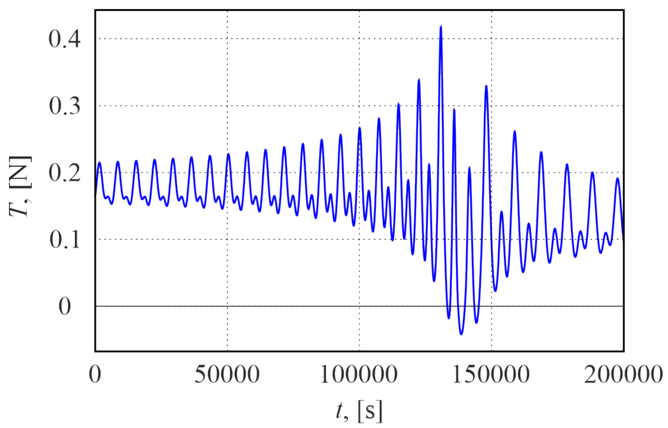

Fig. 12 (**a**) The deflection angles $\theta(t)$, (**b**) the tether length $l(t)$ and (**c**) the tether tension $T(t)$

The sections with negative tension force shown in Fig. 13c indicate that the proposed control law is not feasible using a tether. In these sections, the tether should act like a compressed spring, but it sags ($T<0$). To overcome this difficulty, a low thrust jet propulsion at the end point which thrust is directed along the tether can be used. In these sections the thruster is turned on and implements the required control law (37).

Note the following two facts: first, it takes about 4.6 Earth days for the space elevator to overturn. Secondly, the control law (37) not only makes the space elevator overturn, but also stabilises it in the direction of Mars ($\theta=\pi$).

The space elevator returns to the position oriented towards Phobos (Fig. 13) when the sign of the dimensionless control coefficient changes and with the following initial motion conditions

$$c=200\,,\ \theta_0=-\pi+0.2\,rad\,,\frac{d\theta_0}{dt}=0 \tag{42}$$

(**a**)

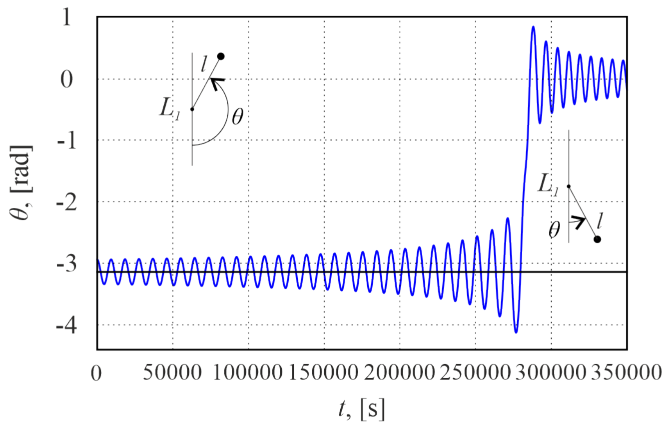

(**b**)

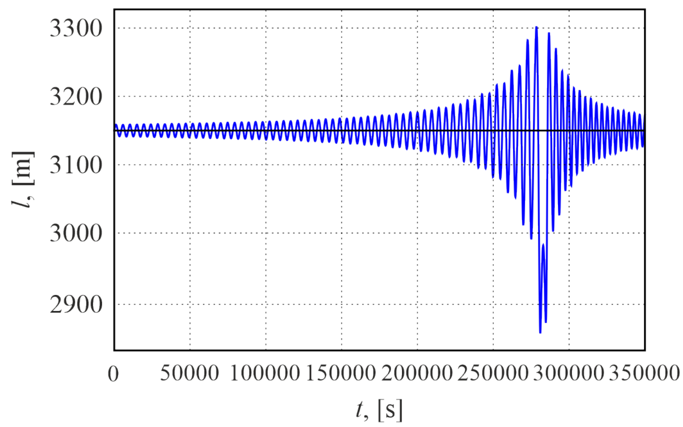

(c)

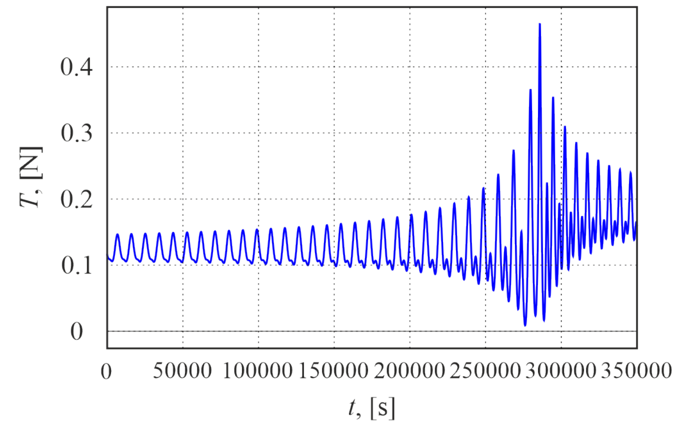

Fig. 13 (**a**) The deflection angles $\theta(t)$, (**b**) the tether length $l(t)$ and (**c**) the tether tension $T(t)$

5 Conclusions

The space elevator deployed from the L1 collinear libration point of the Mars-Phobos system is considered in the framework of the restricted planar circular three-body problem. The main findings of the paper can be summarized in the following way:

1. The motion equations of the space elevator are derived and the control law of the climber velocity is proposed, including accelerating phase, main phase with constant velocity and braking phase.
2. The uniqueness of this space elevator is that it can be deployed from the L1 libration point both towards Phobos for a distance of up to 3.4 km to the surface of Phobos, and towards Mars for a distance of up to several thousand km to the Martian atmosphere.
3. The possibility of turning the space elevator from the direction to Phobos to the direction of Mars and back is illustrated.

This work demonstrates the feasibility of deploying a space elevator from the L1 libration point of the Mars-Phobos system, and of using a climber to move cargo from the surface of Phobos to the space station located at the L1 libration point and back. In the future it will be necessary to

- study the influence of the eccentricity of the Mars-Phobos system orbit on the behaviour of the space lift,
- consider the spatial motion of the space elevator,
- investigate in detail the deployment of such the space elevator to Mars over long distances,
- examine the possibility of using space elevators to transfer satellites to and from quasi-satellite orbits.

Acknowledgements I would like to thank Dr. Alexander Ledkov for helpful discussions of the results.

Data availability The datasets generated during and/oranalyzed during the current study are available from the corresponding author on reasonable request.

Declarations

Conflict of interest The author declares that he has no conflict of interest.

References

1. Beletsky, V.V., Levin, E.M.: Dynamics of space tether systems. Univelt Incorporated, San Diego (1993)
2. Tsiolkovsky, K. E., Speculations Between Earth and Sky, Akademiia Nauk SSSR, Moscow, 1895, p. 35; reprint, Akademiia Nauk SSSR, Moscow, 1959.
3. Artsutanov, Y., “To Space by a Locomotive,” Komsomolskaya Pravda, 31 July 1960.
4. J. Pearson, The orbital tower: a spacecraft launcher using the earth’s rotational energy, Acta Astronautica 2 (1975) 785–799.
5. S.S. Cohen, A.K. Misra, Elastic oscillations of the space elevator ribbon, Journal of Guidance, Control, and Dynamics 30 (2007) 1711–1717.
6. Misra, A.K., Amier, Z., Modi, V.J.: Attitude dynamics of three-body tethered systems. Acta Astronaut. 17(10), 1059–1068 (1988). https://doi.org/10.1016/0094-5765(88)90189-0

7. Woo, P., Misra, A.K.: Dynamics of a partial space elevator with multiple climbers. Acta Astronaut. 67(7–8), 753–763 (2010)

8. P. Woo, A.K. Misra Energy considerations in the partial space elevator Acta Astronautica, 99 (2014), pp. 78-84, 10.1016/j.actaastro.2014.02.013

9. Shi, G., Zhu, Z. & Zhu, Z.H. Libration suppression of tethered space system with a moving climber in circular orbit. Nonlinear Dyn 91, 923–937 (2018). https://doi.org/10.1007/s11071-017-3919-x

10. Shi, G. F., Li, G. Q., Zhu, Z. X., Zhu, Z. H. A virtual experiment for partial space elevator using a novel highfidelity FE model. Nonlinear Dynamics, 2019, 95(4): 2717–2727.

11. Shi, G., & Zhu, Z. H. (2023). Orbital radius keeping of floating partial space elevator in cargo transposition. Astrodynamics, 7(3), 259-269. https://doi.org/10.1007/s42064-022-0156-y

12. Shi, G., & Zhu, Z. H. (2024). New geometric formulation for libration dynamics and suppression of partial space elevator by fuzzy logic and thrust vectoring control. Acta Astronautica. https://doi.org/10.1016/j.actaastro.2024.02.005

13. Jung, W., Mazzoleni, A.P. & Chung, J. Nonlinear dynamic analysis of a three-body tethered satellite system with deployment/retrieval. Nonlinear Dyn 82, 1127–1144 (2015). https://doi.org/10.1007/s11071-015-2221-z

14. Huang, P., Zhang, F., Chen, L. et al. A review of space tether in new applications. Nonlinear Dyn 94, 1–19 (2018). https://doi.org/10.1007/s11071-018-4389-5

15. Yu, B.S., Xu, S.D. & Jin, D.P. Chaos in a tethered satellite system induced by atmospheric drag and Earth’s oblateness. Nonlinear Dyn 101, 1233–1244 (2020). https://doi.org/10.1007/s11071-020-05844-8

16. B.S. Yu, K. Ji, Z.T. Wei, D.P. Jin In-plane global dynamics and ground experiment of a linear tethered formation with three satellites Nonlinear Dynamics, 108 (No. 4) (2022), pp. 3247-3278, 10.1007/s11071-022-07403-9

17. Kumar, K., Yasaka, T.: Rotation formation flying of three satellites using tethers. Journal of Spacecraft and Rockets. 41(6), 973–85 (2004). https://doi.org/10.2514/1.14251

18. Cartmell, M.P., McKenzie, D.J. A review of space tether research. Prog. Aerosp. Sci. 44(1), 1–21 (2008). https://doi.org/10.1016/j.paerosci.2007.08.002

19. Kempton, K., Pearson, J., Levin, E., Carroll, J., & Amzajerdian, F., “Phase 1 Study for the Phobos L1 Operational Tether Experiment (PHLOTE),” End Report, NASA, 2018, pp.1-91. https://ntrs.nasa.gov/search.jsp?R=20190000916.

20. Aslanov, V.S.: Prospects of a tether system deployed at the L1 libration point. Nonlinear Dyn. 106, 2021–2033 (2021). https://doi.org/10.1007/s11071-021-06884-4Пр0.1007/s11071-023-09108-z

21. Aslanov, V.S. A double pendulum fixed at the L1 libration point: a precursor to a Mars–Phobos space elevator. Nonlinear Dyn 112, 775–791 (2024). https://doi.org/10.1007/s11071-023-09108-z

22. Szebehely, V.: The Restricted Problem of Three Bodies, Academic Press Inc., New York (1967)

23. Aslanov, V.S.: Stability of a pendulum with a moving mass: the averaging method. J. Sound Vib. 445, 261–269 (2019). https://doi.org/10.1016/j.jsv.2019.01.021